

Integral behavior for localized synchronization in nonidentical extended systems

J. Bragard^{1,*} and S. Boccaletti²

¹*Department of Physics (B5), University of Liege, 4000 Liege, Belgium*

²*Department of Physics and Applied Mathematics, Universidad de Navarra, Irunlarrea s/n, 31080 Pamplona, Spain*

(Received 24 February 2000)

We report the synchronization of two nonidentical spatially extended fields, ruled by one-dimensional complex Ginzburg-Landau equations. The two fields are prepared in different dynamical regimes, and interact via an imperfect coupling consisting of a given number of local controllers N_c . The strength of the coupling is ruled by the parameter ε . We show that, in the limit of three controllers per correlation length, the synchronization behavior is not affected if the product $\varepsilon N_c/N$ is kept constant, providing a sort of integral behavior for localized synchronization.

PACS number(s): 05.45.Xt, 05.45.Jn, 05.45.Pq

Synchronization of concentrated chaotic systems has been a subject of a large body of recent investigations. In particular, five levels of synchronization have been characterized in this framework, namely, complete synchronization (CS) [1], phase synchronization (PS) [2], lag synchronization (LS) [3], generalized synchronization (GS) [4], and almost synchronization (AS) [5]. CS implies a perfect hooking of the chaotic trajectories of two systems, in such a way as they remain in step with each other in the course of the time. PS is a regime characterized by a quasiperfect locking of the chaotic phases not associated with any correlation in the chaotic amplitudes [2]. LS is an intermediate step between PS and CS. In this case, the two signals lock their phases and amplitudes, but with a finite-time lag [3]. GS implies the hooking of the output of one system to a given function of the output of the other [4]. Finally, AS consists in a regime where only a subset of the variables of one system is completely synchronized with the corresponding subset of variables of the other system [5].

The natural continuation of these pioneering works has been to investigate synchronization phenomena in spatially extended systems. A first approach has been to connect a set of concentrated chaotic systems by means of a given coupling (local or global) between the individuals constituting the set. In this framework, space-time chaos synchronization has been studied for populations of coupled dynamical systems [6], for systems formed by globally coupled Hamiltonian or bistable elements [7], and for neural networks [8]. As for continuous space-time systems, the emergence of synchronized states has been investigated for one-dimensional chemical models [9], and for two fields obeying identical one-dimensional complex Ginzburg-Landau equations [10].

At that point, the obvious question was: Is it possible to realize all different kinds of synchronization features in the case of a coupling between nonidentical extended systems? This problem has been only recently addressed [11–14]. In three previous papers [11,12,15], we have investigated the

synchronization of space-time chaotic states generated by complex Ginzburg-Landau equations (CGLE) as a result of a spatially distributed coupling. The CGLE is known to model the universal pattern forming features close to the emergence of a Hopf bifurcation [16]. It has been used to describe many different situations in laser physics [17], fluid dynamics [18], chemical turbulence [19], bluff body wakes [20], etc.

The system under study is

$$\begin{aligned} \dot{A}_{1,2} = & A_{1,2} + (1 + i\alpha_{1,2})\partial_x^2 A_{1,2} - (1 + i\beta_{1,2})|A_{1,2}|^2 A_{1,2} \\ & + \varepsilon(x)(A_{2,1} - A_{1,2}), \end{aligned} \quad (1)$$

where $A_{1,2}(x,t) \equiv \rho_{1,2}(x,t)\exp[i\psi_{1,2}(x,t)]$ are two complex fields of amplitudes $\rho_{1,2}$ and phases $\psi_{1,2}$, respectively, $\partial_x^2 A_{1,2}$ stays for the second derivative of $A_{1,2}$ with respect to the space variable $0 \leq x \leq L$, L represents the system extension, the dot denotes temporal derivative, $\alpha_{1,2}, \beta_{1,2}$ are suitable real control parameters, $\varepsilon(x)$ rules the strength of the symmetric coupling, and the boundary conditions are chosen to be periodic. In the present paper we deal with localized couplings. We should point out that both in numerical simulations and in practical implementations, a finite resolution in space is unavoidable, leading to a coupling that is extended over a given spatial domain Δ . Therefore, one can reasonably expect that the effect of the coupling depends strongly on the extent of Δ . Since we are interested in studying a coupling whose nature is as localized as possible, we have decided to set Δ equal to the mesh size. This, indeed, represents the maximal spatial resolution that one can obtain in numerical simulations at a given mesh size. In order to provide consistent results, we have kept constant the mesh size all throughout the paper. The detailed study on the dependence of the synchronization features on the selected precision is an important point for practical implementations, and it will be treated in detail elsewhere.

Let us now recall what has been achieved in the previous works; in Ref. [11], we have characterized the synchronization of two identical CGLE ($\alpha_1 = \alpha_2$, $\beta_1 = \beta_2$) as a result of a coupling in a finite number N_c of controllers, which were selected to be equally separated in space ($x_i - x_{i-1} = \xi$). The main result obtained in Ref. [11] is that a finite number of controllers is sufficient to warrant complete synchronization

*Present address: Department of Physics and Center for Interdisciplinary Research on Complex Systems, Northeastern University, Boston, MA 02115.

Email address: jbragard@presto.physics.neu.edu

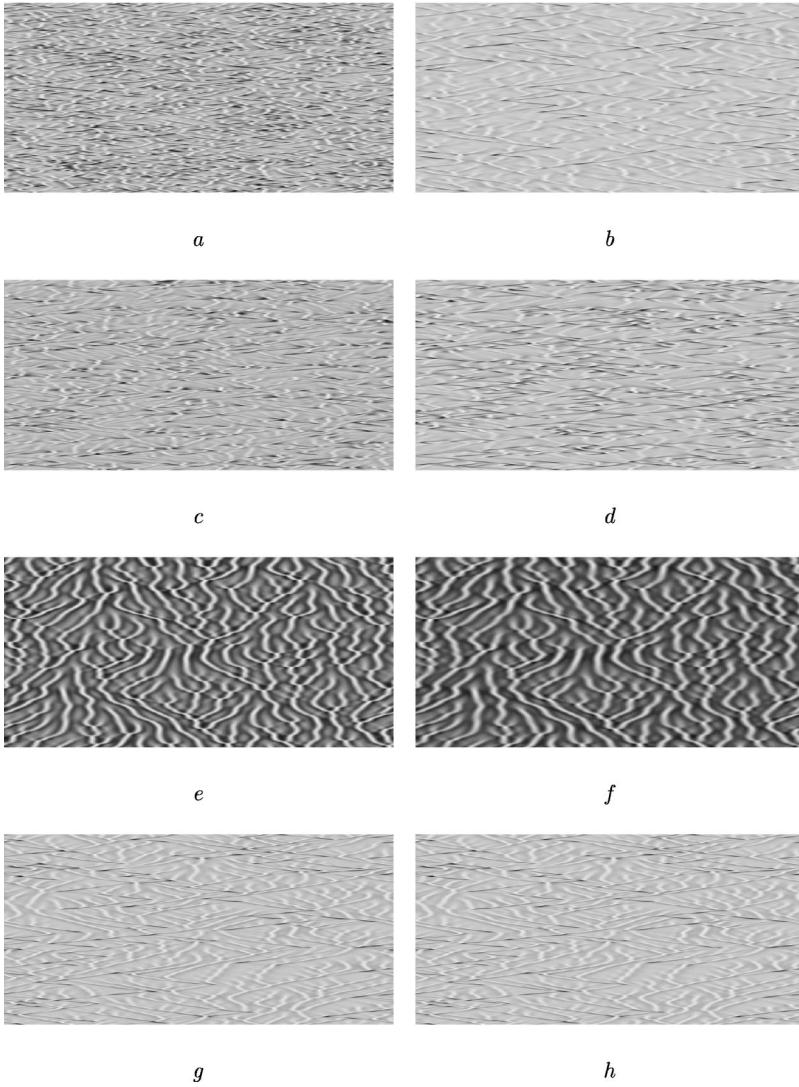


FIG. 1. Case: $N_c = N$: Space (horizontal)-time (vertical) plots of the moduli ρ_1 (a, c, e, g) and ρ_2 (b, d, f, h). $\alpha_1 = \alpha_2 = 2.1$, $\beta_1 = -1.2$, and $\beta_2 = -0.83$. Time increases downwards from 500 to 1500 (u.t.). The first 500 time units (not plotted) after coupling has been started are not represented. Note that the two systems were prepared in two independent chaotic states (AT for A_1 and PT for A_2). (a) and (b) correspond to $\varepsilon = 0.05$, (c) and (d) to $\varepsilon = 0.14$, (e) and (f) to $\varepsilon = 0.2$, and (g) and (h) to $\varepsilon = 2$.

of two identical systems. This kind of phenomenon was proved to be robust up to the limit in which a controller is placed approximately each two correlation lengths ($\xi \leq 2\xi_c$), independently of the mesh size.

In Ref. [12] we were interested in the synchronization of two space-time chaotic fields coming from different dynamics ($\alpha_1 \neq \alpha_2$, $\beta_1 \neq \beta_2$) in the case in which the coupling function was extended on all the N mesh points of the system. The main results coming out from this analysis is a transition for small parameter mismatches from no synchronization to complete synchronization as the local coupling strength increases. At variance, for large parameter mismatches (e.g., if one system lays in the amplitude turbulence regime and the other lays in the phase turbulence regime) the above transition is mediated by a state where a kind of PS was observed. This latter situation was further investigated by us in Ref. [15], where a space-time Fourier analysis indicated that the synchronization phenomenon has rather a temporal behavior than a spatial one and the intermediate stage is the one with larger variations in the mean temporal frequencies of the two systems.

The aim of the present paper is to address two basic questions that were left unanswered in our previous work. The first is how the temporal intermittencies in the spatial average phase differences $\langle \Delta \Psi \rangle_x(t) \equiv \langle |\psi_1(x,t) - \psi_2(x,t)| \rangle_x$

monitored in Ref. [15] can accommodate with a global decrease of the space-time average of the phase differences $\langle \Delta \Psi \rangle \equiv \langle |\psi_1(x,t) - \psi_2(x,t)| \rangle$ observed in Ref. [12]. We will show that the synchronization at large parameter mismatches is deteriorated by a further increase of the coupling between the two systems. The second crucial question is the following: having studied *localized* ($N_c < N$) synchronization between identical systems [11] and *extended* ($N_c = N$) synchronization between nonidentical systems [12,15], is it possible to extend our analysis to the case of a *localized* synchronization between nonidentical systems? Here again, anticipating the results which will follow, the synchronization scenario is not qualitatively affected in the limit $\xi \leq \xi_c$ provided that the coupling strength ε increases *integrally* when the number of controllers decreases, that is the product $\varepsilon N_c / N$ is kept constant.

Let us first illustrate the *integral* behavior of the localized synchronization between two nonequivalent space-time chaotic states. In the uncoupled case [$\varepsilon(x) \equiv 0$] different chaotic regimes can be identified in Eqs. (1) in different regions of the parameter space (α, β) [21], depending on the stability properties of the plane-wave solutions $A_q = \sqrt{1 - q^2} e^{i(qx + \omega t)}$ [$-1 \leq q \leq 1$, q being the wave number in Fourier space, $\omega = -\beta - (\alpha - \beta)q^2$]. In the parameter region

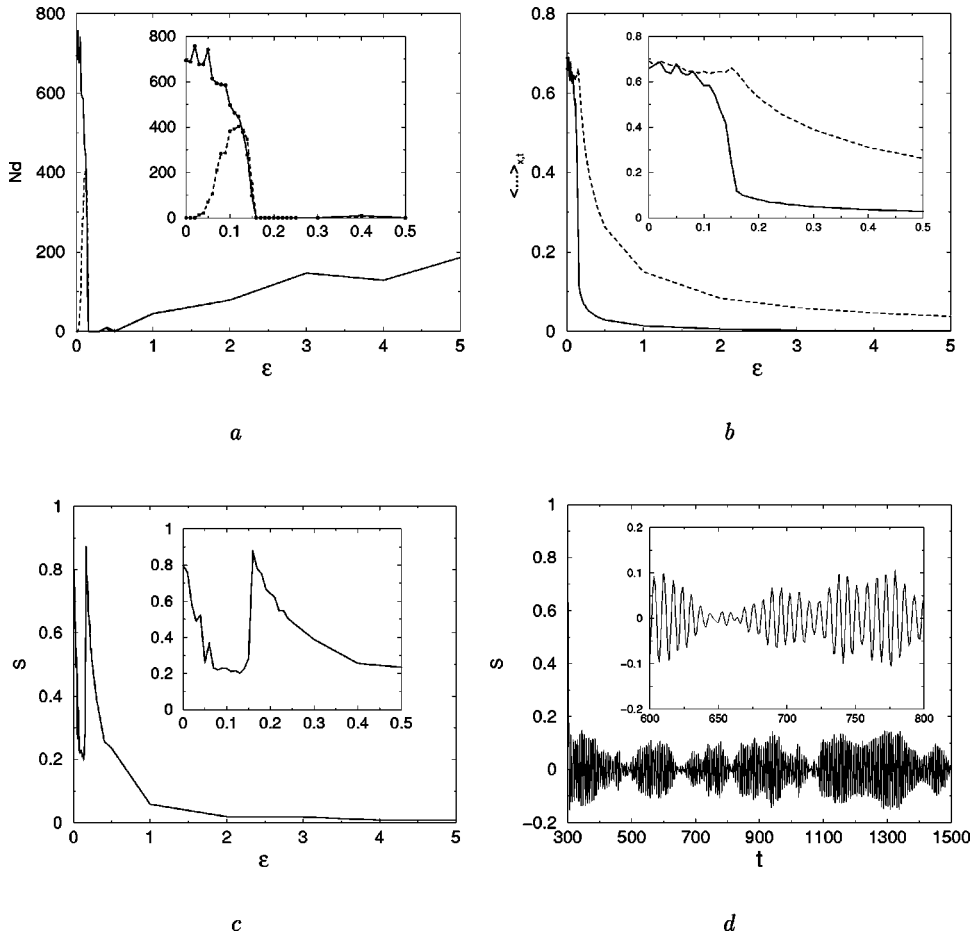


FIG. 2. Case: $N_c=N$: Indicators of synchronization. (a) Total number of defects vs the coupling strength ε for A_1 (solid line) and A_2 (dashed line). The inset reports the zoom at small ε values. (b) The modulus (solid line) and phase (dashed line) indicators vs ε (see the text for definition). The modulus indicator has been multiplied by a factor 7 in order to get the same vertical scale for the two indicators. The inset reports the zoom at small ε values. (c) S indicator (see the text for definition) vs ε . The inset reports the zoom at small ε values. (d) S indicator vs time (in arbitrary units) for a fixed coupling strength $\varepsilon=1$. The inset is a zoom from $t=600$ to $t=800$. Parameters of Eq. (1) are the same as in the caption of Fig. 1.

$\alpha\beta > -1$, there exists a critical value of the wave number $q_c = \sqrt{1 + \alpha\beta/2(1 + \beta^2)} + 1 + \alpha\beta$, such that all the plane waves in the range $-q_c \leq q \leq q_c$ are linearly stable. Outside this range, they become unstable through the so-called Eckhaus instability [22]. Since q_c vanishes as the product $\alpha\beta$ approaches -1 , all plane waves become unstable when crossing from below the so-called Benjamin-Feir line $\alpha\beta = -1$ in the parameter space. Above this line, Ref. [21] identifies three different turbulent regimes, namely, phase turbulence (PT), amplitude turbulence (AT) or defect turbulence, and bichaos. In the following we will concentrate on PT and AT, since they have received special attention in the scientific community [23].

PT is characterized by the fact that the chaotic behavior of the field is essentially dominated by the dynamics of the phase, whereas the amplitude changes smoothly, and it is always bounded away from zero. On the contrary, in AT the amplitude dynamics becomes dominant over the phase dynamics, leading to large amplitude oscillations that can occasionally cause the occurrence of a space-time defect in the point where the amplitude is locally vanishing.

For what was said above, by choosing in Eq. (1) a sufficiently large parameter mismatch between the equations governing the fields $A_{1,2}$, one can select the uncoupled evolutions of A_1 and A_2 to be in AT and PT, respectively (in what follows $\alpha_1 = \alpha_2 = 2.1$, $\beta_1 = -1.2$, and $\beta_2 = -0.83$). The calculated correlation length in the AT case (and for a spatial extension $L=256$) is $\xi_c = 5.38$, for the PT system, there is no exponential decay of the spatial correlation function therefore the correlation length cannot be defined in the usual

sense, still we obtain that $C(x) = 0.5$ for $x \approx 100$. In what follows, we switch on the coupling term on a set of equispaced controllers, and study the synchronization features emerging in the evolution of the two fields, as a function of the two relevant parameters, which are the coupling coefficient ε and the controllers number N_c .

As a first step, we discuss the results of the synchronization between the two states with a coupling coefficient that is active for all mesh points ($N_c=N$). This will serve us as a reference for the following localized case. The numerical method used to integrate Eqs. (1) is a finite difference method with a semi-implicit scheme for the time discretization. The lateral boundary conditions are chosen to be periodic. The spatial extension is $L=256$ and the number of mesh points are $N=2048$. The time step is $\delta_t=0.001$ and the coupling is applied at each time step. Initially, the two systems $A_{1,2}$ are left uncoupled in a Benjamin-Feir unstable plane wave solution during a time $t=1500$ in order to wash out the initial transient and to be in a chaotic AT (for A_1) and PT state (for A_2). After this initial step, the coupling is switched on.

In Fig. 1 we report the patterns arising from the space-time representations of ρ_1 (a, c, e, g) and ρ_2 (b, d, f, h) for $\varepsilon=0.05$ (a, b), $\varepsilon=0.14$ (c, d), $\varepsilon=0.2$ (e, f), $\varepsilon=2$ (g, h). At small coupling strengths, the two systems do not synchronize, and hold in their respective regimes as it is illustrated in Figs. 1(a) and 1(b). At intermediate coupling [Figs. 1(c) and 1(d)], the two systems enter both in a AT state. Some defects ($\rho_2=0$) are created in the system A_2 . For even larger coupling [Figs. 1(e) and 1(f)], the two system return both in a

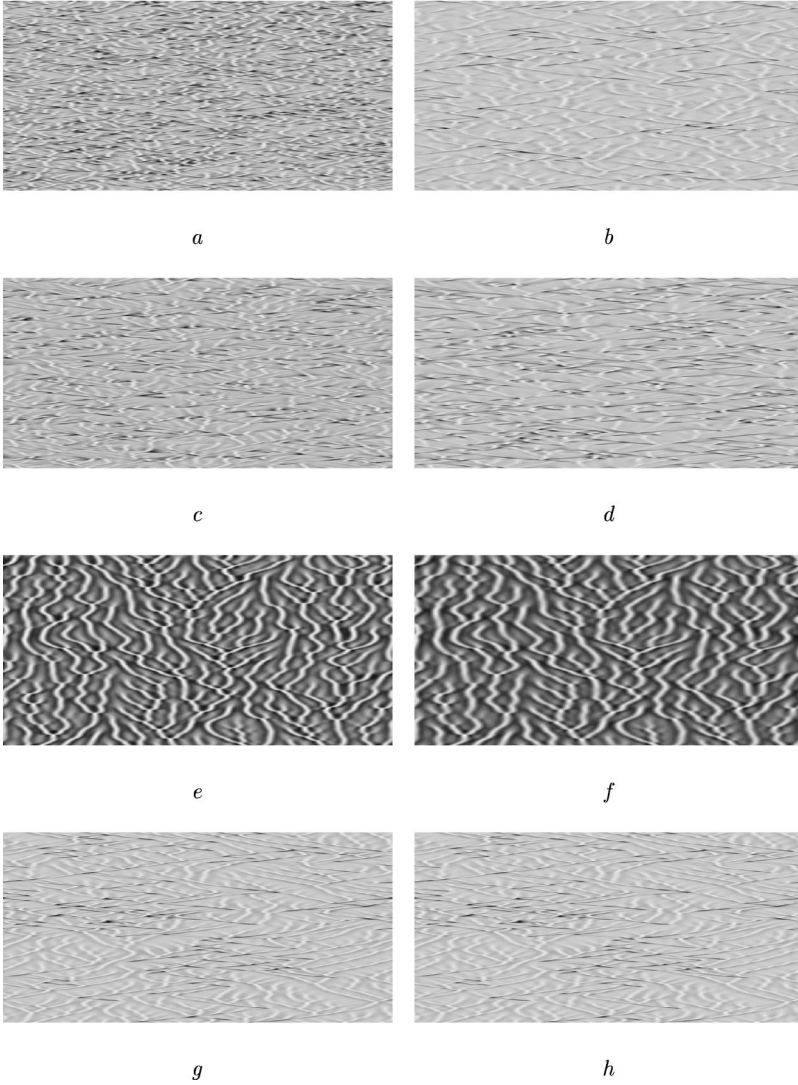


FIG. 3. Case: $N_c = N/5$: Space (horizontal)-time (vertical) plots of the moduli ρ_1 (a, c, e, g) and ρ_2 (b, d, f, h). $\alpha_1 = \alpha_2 = 2.1$, $\beta_1 = -1.2$, and $\beta_2 = -0.83$. Time increases downwards from 500 to 1500 (u.t.). Same general stipulations as in the caption of Fig. 1. (a) and (b) correspond to $\varepsilon = 0.25$, (c) and (d) to $\varepsilon = 0.70$, (e) and (f) to $\varepsilon = 1$, and (g) and (h) to $\varepsilon = 10$.

synchronized PT state, and defects no longer appear in both systems. These three states were already reported by us in Ref. [12], wherein we address the reader for all details. If one further increases the coupling [Figs. 1(g) and 1(h)], the two states hold in a completely synchronized configuration, but there is again creation-annihilation of defects in both systems. A heuristic explanation for this feature is that the two dynamics for A_1 and A_2 are not compatible and the combined dynamics of the synchronized state must deal with this incompatibility by having a ‘‘intermittency’’ type dynamics as it will be illustrated later on.

We now introduce some quantitative indicators for describing the above scenario. In the particular case of two systems, one lying in the AT regime and the other lying in the PT regime, a good indicator for synchronization is the number of defects N_d that are present in each system. Indeed, the PT regime contains no defect as long as it is not coupled to the AT regime, conversely the AT regime that contains defects may eliminate these defects through a coupling with a PT system. Obviously, this indicator cannot be extended in the study of two systems lying both in AT or PT, because in these cases two dynamical systems with the same number of defects do not necessarily follow the same dynamics. In Fig. 2(a), a statistics is made of N_d as a function of ε during $\Delta t = 1000$. The condition for defining a defect is $|\rho| < 0.2$.

The inset reports the situation for small value of the coupling and corresponds to the first three cases of Fig. 1. The number of defects of A_1 is decreasing to zero when the coupling ε is increased. For the system A_2 , the evolution of the number of defects with ε is not monotonous. It increases to a maximum value for $\varepsilon \approx 0.12$, then the number of defects is equal to the number of defects for A_1 and decreases to reach zero when $\varepsilon \approx 0.16$. However, by further increasing the coupling, the number of defects comes out to be again an increasing function of ε (e.g., for $\varepsilon = 2$, $N_d = 79$).

In Fig. 2(b), we plot two others indicators for the synchronization, namely, the average (in space and time) of the modulus difference (solid line)

$$\langle \Delta \rho \rangle = \left\langle \frac{|\rho_1 - \rho_2|}{\rho_1 + \rho_2} \right\rangle_{x,t} \quad (2)$$

and the same average for the phase difference (dashed line)

$$\langle \Delta \psi \rangle = \left\langle \frac{|\psi_1 - \psi_2|}{|\psi_1| + |\psi_2|} \right\rangle_{x,t}. \quad (3)$$

The inset again reports the situation at small coupling values. As it can be clearly seen in Fig. 2(b), the modulus

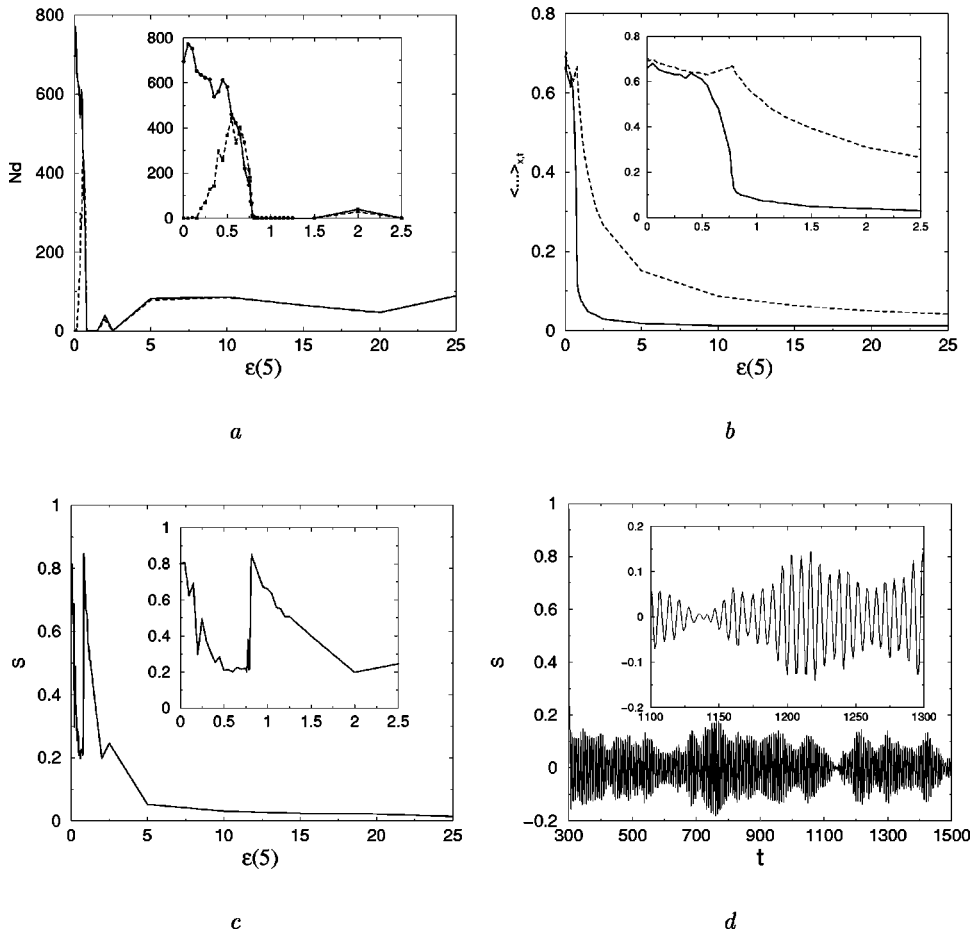


FIG. 4. Case: $N_c = N/5$: Same indicators of synchronization as in Fig. 2. (a) Total number of defects vs the coupling strength ε for A_1 (solid line) and A_2 (dashed line). The inset reports the zoom at small ε values. (b) The modulus (solid line) and phase (dashed line) indicators vs ε . The modulus indicator has been multiplied by a factor 7 in order to get the same vertical scale. The inset reports the zoom at small ε values. (c) S indicator vs ε . The inset reports the zoom at small ε values. (d) S indicator vs time (in arbitrary units) for a fixed coupling strength $\varepsilon = 5$. The inset is a zoom from $t = 1100$ to $t = 1300$. Same parameters as in the caption of Fig. 3. In (a, b, c) $\varepsilon(5)$ means that we take one controller each five mesh points. Notice that the corresponding transitions occur for coupling strengths five times larger than in Fig. 2.

difference decreases much faster than the phase difference, as the coupling increases. This evidence led us to conclude that the defects first synchronize before having a complete synchronization [12]. At larger coupling values both functions decrease but the average phase difference is a very slowly decaying function.

In Figs. 2(c) and 2(d) two different indicators are chosen, namely,

$$S(t, \varepsilon) = \langle \text{Re}(A_1 - A_2) + \text{Im}(A_1 - A_2) \rangle_x \quad (4)$$

and

$$S(\varepsilon) = \langle S(t, \varepsilon) \rangle_t. \quad (5)$$

These indicators are an hybrid between the phase and modulus difference indicators. In Fig. 2(c), we report $S(\varepsilon)$ as a function of the coupling strength. This indicator has the particularity of being not a monotonous function of the coupling parameter ε . In particular, when the number of defects goes to zero, one can observe a sudden increase in the corresponding value of the S indicator. Figure 2(d) reports the temporal evolution of $S(t, \varepsilon)$ at large coupling ($\varepsilon = 2$). From this figure, it becomes evident that the synchronization is not a stable process, and that some kind of intermittency phenomena take place. The two attractors of A_1 and A_2 being not compatible, the dynamics of the combined system is jumping from one to the other in the course of the time.

The effect of a *localized* synchronization is illustrated in Fig. 3, where we represent the space-time plots of ρ_1 (a, c, e,

g) and ρ_2 (b, d, f, h) for $N_c = N/5$. In order to demonstrate that the coupling in the localized case follows an integral behavior, we have chosen $\varepsilon = 0.25$ (a, b), $\varepsilon = 0.70$ (c, d), $\varepsilon = 1$ (e, f), and $\varepsilon = 10$ (g, h) which are exactly five times the coupling strengths used in Fig. 1 for $N_c = N$. Making a comparison with Fig. 1, it is nearly impossible to distinguish between the two scenarios of synchronization stages. A further confirmation for this integral behavior can be obtained

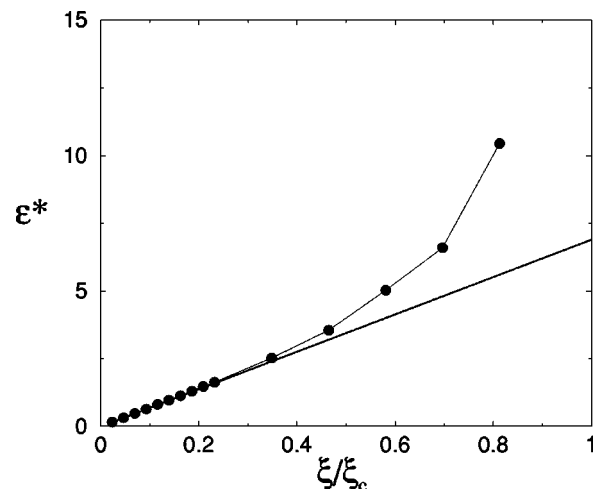


FIG. 5. ε^* (see the text for definition) as a function of the ratio ξ/ξ_c . The straight line aligning the results witnesses the existence of an integral behavior for the localized synchronization in the limit of at least three controllers per spatial correlation length.

by reporting the behavior of the above indicators in the case $N_c = N/5$ (Fig. 4). As it is clear from the figures, the same succession of events occurs for localized synchronization except that the coupling strength has to be multiplied by the factor N_c/N .

To ensure that our results were not casual and also to show up the limitation of this integral behavior, we have performed an ultimate test. We have defined ε^* as the minimum coupling strength for which the number of defects in A_1 and A_2 vanishes, and we have evaluated ε^* at different values of ξ/ξ_c . In all cases the controllers are equally separated in space from each other with a separation ξ and ξ_c is the correlation length of the AT system, which is by far the smaller of the two systems. Furthermore, we have limited our analysis to the case of at least one controller for spatial correlation length, since, as already discussed above, the lack of robustness in the synchronization properties at larger ratios ξ/ξ_c was already demonstrated by us in Ref. [11]. The outcome of this test is summarized in Fig. 5, where the integral behavior is witnessed by the fact that the results align quasiperfectly on a straight line for a value of $\xi/\xi_c < 1/3$. When the number of controllers decreases, the integral be-

havior no longer holds and the synchronization between the two systems is obtained for the larger value of the coupling constant ε . A similar scenario appears in Ref. [24].

We do not want to claim that the number 1/3 is universal but it presumably depends on the characteristic parameters of the two considered systems.

In summary, we have discussed the case of a coupling between two systems with different dynamical properties with a finite number of controllers. The main conclusion is that synchronization is robust even in this case, and follows an integral behavior in the limit of at least three controllers per spatial correlation length.

We are indebted to H. Mancini, D. Maza, F. T. Arecchi, J. Kurths, and A. Pikovsky for many useful discussions. This work was partly supported by Integrated Action Italy-Spain HI97-30. S.B. acknowledges financial support from the EU through Contract No. ERBFMBICT983466. This text presents results of the Belgian Program Inter-University Pole of Attraction (IUPA IV-06) initiated by the Belgian State, Prime Minister's Office, Federal Office for Scientific, Technical and Cultural Affairs.

-
- [1] L.M. Pecora and T.L. Carroll, Phys. Rev. Lett. **64**, 821 (1990).
 [2] M.G. Rosenblum, A. Pikovsky, and J. Kurths, Phys. Rev. Lett. **76**, 1804 (1996).
 [3] M.G. Rosenblum, A. Pikovsky, and J. Kurths, Phys. Rev. Lett. **78**, 4193 (1997).
 [4] N.F. Rulkov, M.M. Sushchik, L.S. Tsimring, and H.D.I. Abarbanel, Phys. Rev. E **51**, 980 (1995).
 [5] R. Femat and G. Solis-Perales, Phys. Lett. A **262**, 50 (1999).
 [6] A. Pikovsky, M.G. Rosenblum, and J. Kurths, Europhys. Lett. **34**, 165 (1996).
 [7] D.H. Zanette, Phys. Rev. E **55**, 5315 (1997).
 [8] D.H. Zanette and A.S. Mikhailov, Phys. Rev. E **58**, 872 (1998).
 [9] P. Parmananda, Phys. Rev. E **56**, 1595 (1997).
 [10] A. Amengual, E. Hernández-García, R. Montagne, and M. San Miguel, Phys. Rev. Lett. **78**, 4379 (1997).
 [11] S. Boccaletti, J. Bragard, and F.T. Arecchi, Phys. Rev. E **59**, 6574 (1999).
 [12] S. Boccaletti, J. Bragard, F.T. Arecchi, and H.L. Mancini, Phys. Rev. Lett. **83**, 536 (1999).
 [13] H. Chaté, A. Pikovsky, and O. Rudzick, Physica D **131**, 17 (1999).
 [14] L. Junge and U. Parlitz, Phys. Rev. Lett. (to be published).
 [15] J. Bragard, F.T. Arecchi, and S. Boccaletti, Int. J. Bifurcation Chaos Appl. Sci. Eng. (to be published).
 [16] M. Cross and P. Hohenberg, Rev. Mod. Phys. **65**, 851 (1993), and reference therein.
 [17] P. Couillet, L. Gil, and F. Roca, Opt. Commun. **73**, 403 (1989).
 [18] P. Kolodner, S. Slimani, N. Aubry, and R. Lima, Physica D **85**, 165 (1995).
 [19] Y. Kuramoto and S. Koga, Prog. Theor. Phys. Suppl. **66**, 1081 (1981).
 [20] T. Leweke and M. Provansal, Phys. Rev. Lett. **72**, 3174 (1994).
 [21] B. Shraiman, A. Pumir, W. van Saarloos, P.C. Hohenberg, H. Chate, and M. Holen, Physica D **57**, 241 (1992); H. Chaté, Nonlinearity **7**, 185 (1994); in *Spatiotemporal Patterns in Nonequilibrium Complex Systems*, edited by P.E. Cladis and P. Palfy-Muhoray (Addison-Wesley, New York, 1995).
 [22] B. Janiaud, A. Pumir, D. Bensimon, V. Croquette, H. Richter, and L. Kramer, Physica D **55**, 269 (1992).
 [23] H. Sakaguchi, Prog. Theor. Phys. **84**, 792 (1990); D. Egolf and H. Greenside, Nature (London) **369**, 129 (1994); R. Montagne, E. Hernández-García, and M. San Miguel, Phys. Rev. Lett. **77**, 267 (1996); A. Torcini, *ibid.* **77**, 1047 (1996); M. van Hecke, *ibid.* **80**, 1896 (1998).
 [24] R.O. Grigoriev, M.C. Cross, and H.G. Schuster, Phys. Rev. Lett. **79**, 2795 (1997).